A Density Functional Theory Analysis of the relationships between electronic structure and KCNQ2 potassium channels inhibition by a series of retigabine derivatives

Juan S. Gómez-Jeria[1]*, Gaston A. Kpotin[2]

[1]Quantum Pharmacology Unit, Department of Chemistry, Faculty of Sciences, University of Chile. Las Palmeras 3425, Ñuñoa, Santiago 7800003, Chile

[2]Laboratory of Theoretical Chemistry and Molecular Spectroscopy, Faculty of Sciences and Technique, University of Abomey-Calavi, 03 BP 3409 Cotonou-Benin

Abstract A quantum-chemical analysis of the relationships between electronic structure and KCNQ2 potassium channels inhibition was carried out for a group of retigabine derivatives. For the quantitative structure-activity relationship (QSAR) investigation, we have employed the Klopman-Peradejordi-Gómez formal method. A statistically significant equation, relating the variation of the inhibitory capacity to the variation of the numerical value of several local atomic reactivity indices was found. The mechanism of action is orbital-controlled. The obtained results allowed building the partial 2D pharmacophore that should be useful to design new derivatives with enhanced inhibitory capacity.

Introduction

A recent study showed that a centipede (*Scolopendra subspinipes mutilans*, that weighs around 3 g) can subdue a mouse that weighs around about 45 g within 30 seconds [1]. This capacity of subduing giant preys is due to a peptide toxin, called SsTx, which blocks KCNQ potassium channels, causing disorders in the cardiovascular, nervous and respiratory systems. The study also demonstrated that a KCNQ/Kv7 opener, retigabine (Ethyl *N*-[2-amino-4-[(4-fluorophenyl)methylamino]phenyl]carbamate), neutralizes the toxicity of a centipede's venom. Therefore, the search of retigabine derivatives with an enhanced capacity to neutralize the centipede's venom should be a priority task. In 2013 Gao, Nan et al. published a study of several retigabine derivatives that inhibits KCNQ2 potassium channels [2].

This topic interested us enough to use Gao, Nan et al. molecules for a theoretical investigation of the relationships between the electronic structure and the inhibition of potassium channels. In this paper we present the results of this study employing the Klopman-Peradejordi-Gómez (KPG) method.

Methods, models and calculations [3]

The method

Within the Klopman-Peradejordi-Gómez (KPG) method, a biological activity BA is a function of several local atomic reactivity indices (LARIs) and has the following general linear form [4-9]:

$$\log(BA)_i \cong a + bM_{D_i} + c\log\left[\sigma_{D_i}/(ABC)^{1/2}\right] + \sum_j\left[e_jQ_j + f_jS_j^E + s_jS_j^N\right] +$$

$$+ \sum_j\sum_m\left[h_j(m)F_j(m) + x_j(m)S_j^E(m)\right] + + \sum_j\sum_{m'}\left[r_j(m')F_j(m') + t_j(m')S_j^N(m')\right] +$$

$$+ \sum_j\left[g_j\mu_j + k_j\eta_j + o_j\omega_j + z_j\varsigma_j + w_jQ_j^{max}\right] \tag{1}$$

where M is the drug's mass, σ its symmetry number and ABC the product of the drug's moment of inertia about the three principal axes of rotation, Q_i is the net charge of atom i, S_i^E and S_i^N are, respectively, the total atomic electrophilic and nucleophilic superdelocalizabilities of atom i, $F_{i,m}$ is the Fukui index of the occupied (empty) MO m (m') localized on atom i. $S_i^E(m)$ is the atomic electrophilic superdelocalizability of MO m on atom i, etc. S_i^E is defined as the sum over occupied MOs of the $S_i^E(m)$'s and S_i^N is defined as the sum over empty MOs of the $S_i^N(m)$'s. The last bracket of the right side of Eq. 1 contains new local atomic reactivity indices obtained within the Hartree-Fock scheme. The local atomic electronic chemical potential of atom i, μ_i, is defined as:

$$\mu_i = \frac{E_{oc}^* - E_{em}^*}{2} \tag{2}$$

where E_{oc}^* is the upper occupied MO localized on atom i having a non-zero Fukui index (called HOMO*) and E_{em}^* is the lowest empty MO localized on atom i having a non-zero Fukui index (called LUMO*). These molecular orbitals are called local frontier molecular orbitals because in many cases they do not coincide with the molecule's frontier MOs. The total local atomic hardness of atom i, η_i, is defined as:

$$\eta_i = E_{em}^* - E_{oc}^* \tag{3}$$

and corresponds to the HOMO*-LUMO* gap. The total local atomic softness of atom i, ς_i, is defined as the inverse of the local atomic hardness. The local electrophilic index of atom i, ω_i, is defined as:

$$\omega_i = \frac{\mu_i^2}{2\eta_i} \tag{4}$$

The maximal amount of electronic charge that an electrophile may accept, Q_i^{max}, is defined as:

$$Q_i^{max} = \frac{-\mu_i}{\eta_i} \tag{5}$$

These are the local atomic analogues of similar global reactivity indices. Note that these indices have the same physical units that their global counterparts. They are conceptually different from the projected indices obtained within conceptual Density Functional Theory. μ_i is the middle point between the HOMO$_i$* and LUMO$_i^*$, and it is a measure of the tendency of an atom to gain or lose electrons; a large negative value indicates a good electron acceptor atom while a small negative value implies a good electron donor atom. The local atomic hardness can be interpreted as the resistance of an atom to exchange electrons with the environment. In fact η_i is the HOMO$_i$*-LUMO$_i$* gap. The local atomic electrophilic index is associated with the electrophilic power of an atom and includes the tendency of the electrophile atom to receive extra electronic charge together with its resistance to exchange charge with the medium.

The fundamental importance of Eq. 1 is that it contains only terms belonging to the drug molecules. For the case of biological activities that are not affinity constants it is required that the experimental measurements be carried out in almost identical way(s) and that all the molecules considered have exactly the same action mechanism. Therefore, for n (i=1,N) molecules we have a set of simultaneous equations 1. This system of simultaneous equations holds for

the atoms of the molecule directly involved in the interaction process. Combined with the standard multiple-regression techniques, these equations can be usefully applied to estimate the relative variation of the biological activities in the family of molecules analyzed. The KPG method has shown its utility for many different molecular systems and biological activities [10-14].

Selection of molecules and biological activities

The molecules were selected from a recent study [2]. Their general formula and biological activity are displayed, respectively, in Fig. 1 and Table 2.The reported biological property was obtained using the whole-cell patch clamp technique and corresponds to the ratio between the amplitude of the outward current in the presence of the compound (I) and the amplitude of the outward current in the absence of the compound (I_0). Compounds with $I/I_0 > 1$ are defined as activators, while compounds with $I/I_0 < 1$ were defined as inhibitors.
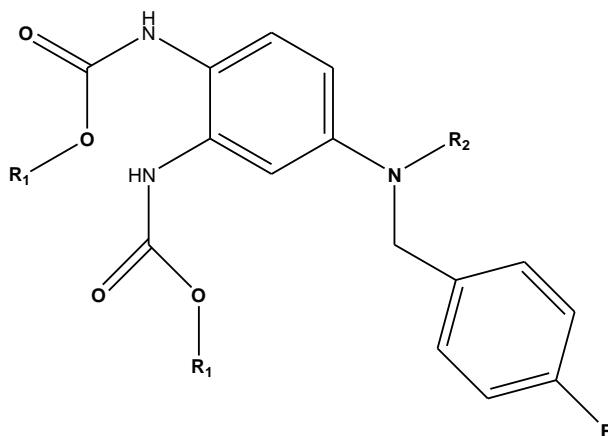
Figure 1: General formulas of retigabine derivatives

Table 1: Retigabine derivatives and effects on KCNQ2 channels

Mol.	Mol.	R_1	R_2	I/I_0	$\log_{10}(I/I_0)$
1	HN31	Et	Me	1.55	0.19
2	HN32	Et	Et	1.17	0.07
3	HN33	Et	n-Pr	0.28	-0.55
4	HN34	Et	n-Pen	0.36	-0.44
5	HN35	Et	n-Bu	1.01	0.00
6	HN36	Et	$CH_2CH=CHMe$	0.87	-0.06
7	HN37	Et	$CH_2CH=C(Me)_2$	0.66	-0.18
8	HN38	Et	$CH_2C(Me)=CH_2$	0.08	-1.10
9	HN39	Et	$CH_2C(=CH_2)(CH_2)_7Me$	1.18	0.07
10	HN310	Et	$CH_2C(=CH_2)C(=O)OMe$	0.24	-0.62
11	HN311	Et	$CH_2CH_2C(=CH_2)Me$	0.29	-0.54
12	HN41	Me	$CH_2CH_2C(=CH_2)Me$	1.43	0.16
13	HN42	n-Pr	$CH_2CH_2C(=CH_2)Me$	0.16	-0.80
14	HN43	Allyl	$CH_2CH_2C(=CH_2)Me$	0.24	-0.62
15	HN44	i-Bu	$CH_2CH_2C(=CH_2)Me$	0.5	-0.30
16	HN45	t-Bu	$CH_2CH_2C(=CH_2)Me$	1.24	0.09
17	HN46	Me	$CH_2C(=CH_2)Me$	1.14	0.06
18	HIT1	Et	$CH_2CH=CH_2$	0.3	-0.52
19	HN47	n-Pr	$CH_2C(=CH_2)Me$	0.27	-0.57
20	HN48	Allyl	$CH_2C(=CH_2)Me$	0.17	-0.77
21	HN49	i-Pr	$CH_2C(=CH_2)Me$	0.24	-0.62
22	HN410	i-Bu	$CH_2C(=CH_2)Me$	1.08	0.03

Calculations

The electronic structure of all molecules was calculated with the Density Functional Theory at the B3LYP/6-31g(d,p) level after full geometry optimization. The Gaussian collection of programs was used [15]. All the data used to calculate numerical values for the local atomic reactivity indices was obtained from the Gaussian results with the D-CENT-QSAR software [16]. All electron populations smaller than or equal to 0.01 e were considered as zero. Negative electron populations coming from Mulliken Population Analysis were rectified as habitual [17]. Given that the number of molecules is not enough to solve the system of linear equations; we made use of Linear Multiple Regression Analysis (LMRA) techniques to find the best set of local atomic reactivity indices whose variation gives a significant account of the variation of the biological activity under study. For each case, a matrix containing the dependent variable (the biological activity of each case) and the local atomic reactivity indices of all atoms of the common skeleton as independent variables was built. The Statistica software was used for LMRA [18]. We worked using the *common skeleton hypothesis* stating that there is a definite collection of atoms, common to all molecules analyzed, that accounts for nearly all the biological activity. The action of the substituents consists in modifying the electronic structure of the common skeleton and influencing the right alignment of the drug. It is conjectured that different parts or this common skeleton accounts for almost, but not all the interactions leading to the expression of a given biological activity [6]. The common skeleton for retigabine derivatives is shown in Fig. 2.
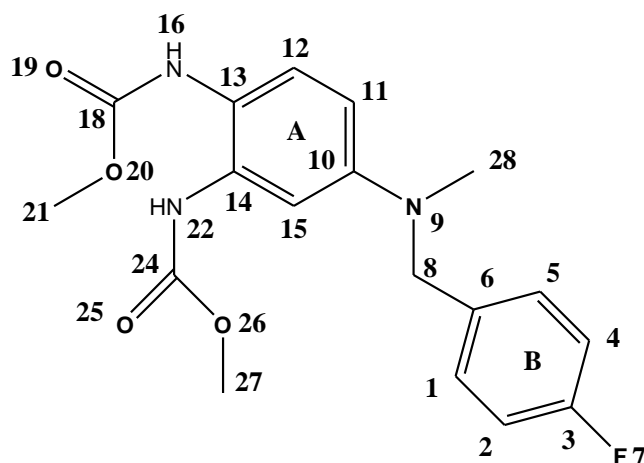
Figure 2: Common skeleton of retigabine derivatives

Results

The best equation obtained was:

$$\log(I/I_0) = -1.68 + 0.14\eta_{27} - 0.001 S_{10}^N(\text{LUMO}+2)^* - 0.11 S_{21}^N(\text{LUMO}+1)^* -$$
$$-3.68 F_{28}(\text{LUMO}+2)^* + 1.75 S_{10}^E(\text{HOMO}-1)^* + 3.11 s_{22}$$

(6)

with n=22, R=0.96, R^2=0.91, adj-R^2=0.88, F(6,15)=25.958 (*p*<0.000001) and SD=0.13. No outliers were detected and no residuals fall outside the ±2σ limits. Here, η_{27} is the local atomic hardness of atom 27, $S_{10}^N(\text{LUMO}+2)^*$ is the nucleophilic superdelocalizability of the third lowest empty local MO of atom 10, $S_{21}^N(\text{LUMO}+1)^*$ is the nucleophilic superdelocalizability of the second lowest empty local MO of atom 21, $F_{28}(\text{LUMO}+2)^*$ is the electron population of the third lowest empty local MO of atom 28, $S_{10}^E(\text{HOMO}-1)^*$ is the electrophilic superdelocalizability of the second highest occupied local MO of atom 10 and s_{22} is the local atomic softness of atom 22. Tables 2 and 3 show the beta coefficients, the results of the t-test for significance of coefficients and the matrix of squared correlation coefficients for the variables of Eq. 1. There are no significant internal correlations between independent variables (Table 3). Figure 3 displays the plot of observed *vs.* calculated $\log(I/I_0)$.

Table 2: Beta coefficients and t-test for significance of coefficients in Eq. 1

	Beta	**t(15)**	**p-level**
η_{27}	0.44	5.47	0.00006
$S_{10}^{N}(LUMO+2)^*$	-0.78	-9.04	0.000000
$S_{21}^{N}(LUMO+1)^*$	-0.46	-5.57	0.00005
$F_{28}(LUMO+2)^*$	-0.29	-3.59	0.003
$S_{10}^{E}(HOMO-1)^*$	0.24	3.01	0.009
s_{22}	0.23	2.69	0.02

Table 3: Matrix of squared correlation coefficients for the variables in Eq. 1

	η_{27}	$S_{10}^{N}(LUMO+2)^*$	$S_{21}^{N}(LUMO+1)^*$	$F_{28}(LUMO+2)^*$	$S_{10}^{E}(HOMO-1)^*$
$S_{10}^{N}(LUMO+2)^*$	0.00	1.00			
$S_{21}^{N}(LUMO+1)^*$	0.06	0.04	1.00		
$F_{28}(LUMO+2)^*$	0.01	0.01	0.03	1.00	
$S_{10}^{E}(HOMO-1)^*$	0.00	0.09	0.00	0.01	1.00
s_{22}	0.03	0.11	0.00	0.03	0.02
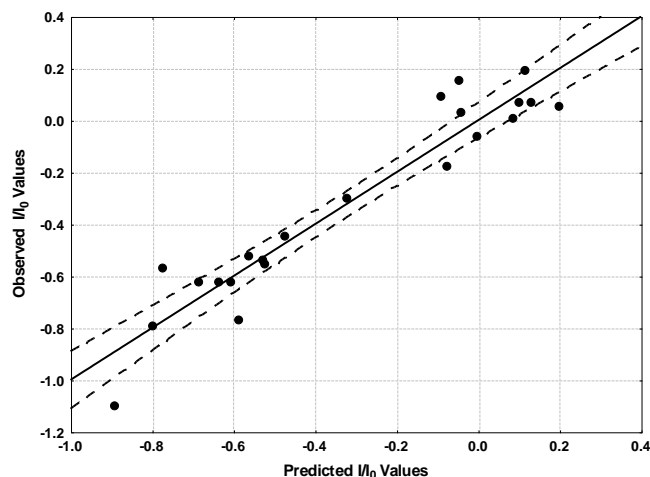
Figure 3: Plot of predicted vs. observed log(I/I_0) values (Eq. 1). Dashed lines denote the 95% confidence interval

The associated statistical parameters of Eq. 1 indicate that this equation is statistically significant and that the variation of the numerical values of a group of six local atomic reactivity indices of atoms of the common skeleton explains about 88% of the variation of $\log(I/I_0)$ in this group of retigabine derivatives. Figure 3, spanning about 1.3 orders of magnitude, shows that there is a good correlation of observed *versus* calculated values and that almost all points are inside the 95% confidence interval. It is important to mention that the descriptors (i.e., the local atomic reactivity indices) are not normalized because they have a concrete physical meaning and units (e, eV, etc.). Therefore the coefficients are not normalized. This is necessary for keeping the physics of the equation and also for comparison with other studies carried out with different molecules interacting with the same receptors. Also, the KPG method has not the obligation to perform the external and internal validation because of its mathematical formal structure. Another very important point to stress is the following. In the case of large molecules the HOMO, and all the remaining MOs, could be localized only on one set of atoms (exception are the core MOs). Now, when we define the *local* molecular orbitals of a given atom, we use only those molecular MOs localized on it. This implies that each atom in a large molecule must have its own complete set of HOMO*, (HOMO-1)*, LUMO*, (LUMO+1)*, etc. For this reason, when a local atomic reactivity index of an inner occupied MO (i.e., HOMO-1 and/or HOMO-2) or of a higher vacant MO (LUMO+1 and/or LUMO+2) appears in any equation, this means that the remaining of the upper occupied MOs (for example, if HOMO-2 appears, upper means HOMO-1 and HOMO) or the remaining of the empty MOs (for example, if LUMO+1 appears, lower means the LUMO) contribute to the

biological activity. Their absence in the equation only means that the variation of their numerical values does not account for the variation of the numerical value of the biological property.

Local Molecular Orbitals

Tables 4 and 5 display the local molecular orbital structure of all atoms appearing in Eq. 1.Nomenclature of the Tables: Molecule (HOMO number) / (HOMO-2)* (HOMO-1)* (HOMO)* - (LUMO)* (LUMO+1)* (LUMO+2)*.

Table 4: Local molecular orbitals of atoms 10, 21 and 22

Mol.	Mol.	Atom 10 (C)	Atom 21 (C)	Atom 22 (N)
HN31	1 (103)	99π101π103π-105π107π108π	97σ100σ101σ-107σ109σ114σ	101π102π103π-105σ108π116σ
HN32	2 (107)	102π104π107π-109π111π112π	97σ98σ99σ-116σ117σ119σ	104π106π107π-113π114σ119σ
HN33	3 (111)	109π110π111π-112π113π114π	94σ101σ102σ-118σ119σ120σ	106σ110π111π-113σ117σ144σ
HN34	4 (119)	111π114π119π-123π124π125π	99σ100σ110σ-127σ128σ132σ	117π118π119π-121π125π126π
HN35	5 (115)	105π112π115π-119π120π121π	105σ107σ108σ-123σ125σ129σ	113π114π115π-117σ120π129σ
HN36	6 (114)	111π113π114π-115π116π117π	103σ105σ106σ-130σ132σ134σ	111π113σ114π-120σ124σ128σ
HN37	7 (118)	116π117π118π-119π120π121π	108σ109σ110σ-134σ135σ138σ	116π117π118π-124σ135σ136σ
HN38	8 (114)	112π113π114π-115π116π118π	103σ105σ106σ-130σ131σ135σ	111π113π114π-116σ120σ129σ
HN39	9 (142)	139σ141π142π-143π145π146π	131σ132σ133σ-151σ152σ155σ	140π141π142π-143σ148σ165σ
HN310	10 (125)	123π124π125π-126σ127π128π	114σ115σ116σ-138σ143σ144σ	123π124π125π-127σ131σ134σ
HN311	11 (118)	115π116π118π-121π122π123π	107σ108σ110σ-125σ129σ134σ	115π116π117π-124σ126σ130σ
HN41	12 (102)	99π101π102π-103π104π105π	91σ93σ94σ-113σ114σ115σ	100π101π102π-108π112σ117σ
HN42	13 (118)	116π117π118π-120π121π122π	107σ109σ110σ-128σ129σ131σ	112π117π118π-120π124σ133σ
HN43	14 (116)	109σ113π116π-120π121π122π	105σ108σ112σ-120σ121σ123σ	114π115π116π-118σ124σ133σ
HN44	15 (126)	123π125π126π-128π129π130π	113σ115σ116σ-134σ135σ138σ	124π125π126π-132σ138σ142σ
HN45	16 (126)	122π124π126π-127π129π130π	116σ117σ119σ-132σ134σ137σ	124π125π126π-130π133σ134σ
HN46	17 (106)	100π105π106π-107π108π109π	90σ91σ97σ-114σ117σ119σ	101σ105π106π-108π113π118σ
HIT1	18 (114)	103π111π114π-116π117π118π	103σ105σ106σ-126σ130σ131σ	112π113π114π-116σ120σ129σ
HN47	19 (122)	120π121π122π-123π124π126π	111σ113σ114σ-132σ133σ135σ	119π121π122π-124σ128σ138σ
HN48	20 (120)	117σ119π120π-122π123π124π	105σ108σ116σ-127σ131σ139σ	112π119π120π-123π129σ132σ
HN49	21 (122)	119σ120π122π-123π124π125π	113σ114σ116σ-131σ137σ138σ	118π121π122π-128σ132σ138σ
HN410	22 (130)	124σ126π130π-132π133π134π	120σ121σ122σ-141σ142σ143σ	128π129π130π-132σ137σ143σ

Table 5: Local molecular orbitals of atoms 27 and 28

Mol.	Mol.	Atom 27 (C)	Atom 28 (C)
HN31	1 (103)	88σ89σ94σ-111σ112σ114σ	99σ102σ103σ-111σ115σ118σ
HN32	2 (107)	96σ99σ100σ-120σ121σ122σ	97σ102σ107σ-115σ117σ119σ
HN33	3 (111)	104σ105σ106σ-113σ117σ119σ	109σ110σ111σ-113σ115σ120σ
HN34	4 (119)	112σ113σ116σ-123σ125σ128σ	109σ114σ119σ-128σ129σ130σ
HN35	5 (115)	99σ100σ106σ-123σ125σ128σ	105σ112σ115σ-125σ126σ129σ
HN36	6 (114)	98σ104σ107σ-122σ123σ128σ	111σ112σ113σ-119σ127σ128σ
HN37	7 (118)	107σ108σ111σ-125σ127σ128σ	114σ115σ117σ-122σ123σ132σ
HN38	8 (114)	103σ104σ107σ-121σ123σ124σ	110σ111σ112σ-119σ127σ129σ
HN39	9 (142)	132σ133σ135σ-149σ151σ153σ	138σ139σ142σ-143σ145σ146σ
HN310	10 (125)	109σ112σ118σ-131σ135σ141σ	122σ123σ124σ-130σ133σ139σ
HN311	11 (118)	113σ114σ117σ-124σ129σ132σ	114σ115σ118σ-121σ122σ123σ
HN41	12 (102)	91σ92σ95σ-110σ111σ117σ	97σ99σ100σ-107σ114σ115σ
HN42	13 (118)	108σ109σ111σ-124σ125σ126σ	115σ116σ118σ-120σ122σ123σ
HN43	14 (116)	104σ107σ110σ-120σ121σ123σ	103σ109σ113σ-119σ122σ127σ
HN44	15 (126)	114σ116σ117σ-134σ135σ137σ	124σ125σ126σ-129σ130σ131σ
HN45	16 (126)	117σ118σ123σ-133σ138σ140σ	121σ122σ126σ-131σ138σ140σ
HN46	17 (106)	95σ96σ99σ-114σ115σ116σ	103σ104σ106σ-108σ109σ110σ
HIT1	18 (114)	102σ104σ107σ-120σ123σ124σ	103σ110σ111σ-119σ123σ127σ
HN47	19 (122)	112σ113σ115σ-128σ129σ131σ	118σ119σ120σ-127σ135σ136σ
HN48	20 (120)	109σ111σ113σ-124σ125σ133σ	117σ118σ120σ-122σ124σ126σ
HN49	21 (122)	109σ112σ115σ-128σ131σ134σ	111σ118σ119σ-126σ127σ135σ
HN410	22 (130)	123σ125σ126σ-137σ142σ144σ	124σ127σ130σ-135σ144σ145σ

Discussion

The molecular electrostatic potential (MEP) is a good guide in assessing the molecules' reactivity towards positively or negatively charged reactants. We have refined Ariens' model of the space surrounding the receptor site and suggested that, at a distance where weak/medium ligand-site interactions (4-5 Å) are in action, the orientation and guiding processes probably begins. Figure 4 show the MEP maps of molecules HN31 and HN41, the best activators

of the set (Table 1). Figure 5 show the MEP maps of molecules HN38 and HN42, the best inhibitors (Table 1). The maps are drawn at 4.5 Å of the nuclei [19].
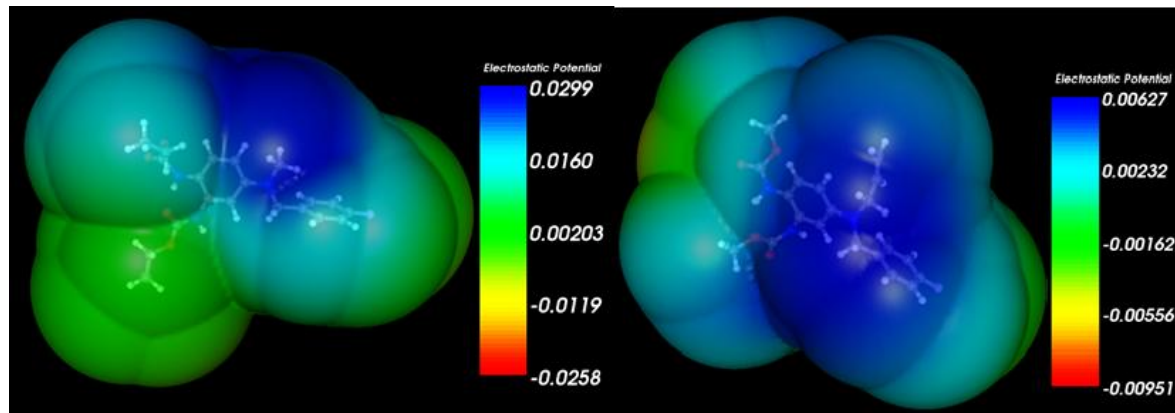
Figure 4: MEP map of molecules HN31 (left) and HN41 (right)
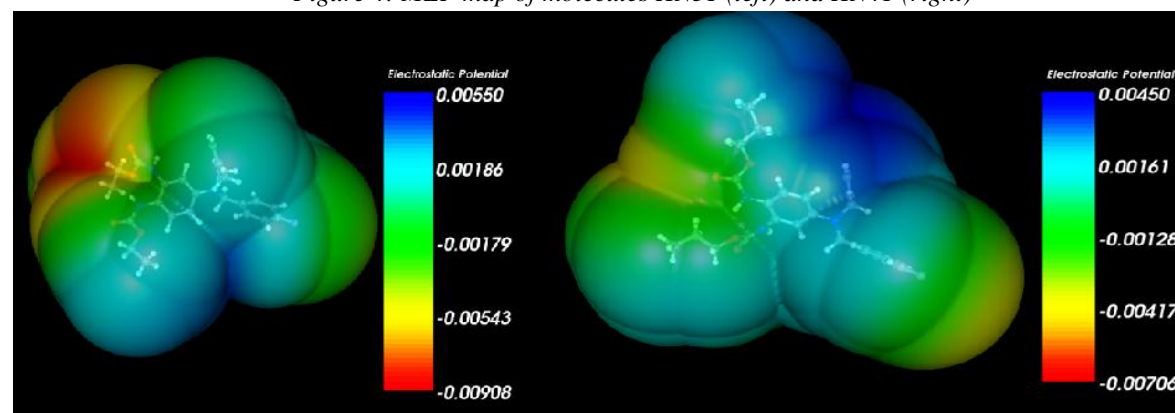
Figure 5: MEP map of molecules HN38 (left) and HN42 (right)

The negative regions are close to the two carboxylic regions. The other negative MEP region is due to the fluorine substituent in ring B (see Fig. 2). All the MEP maps were calculated for the minimum energy conformation of each molecule. This conformation is not necessarily the active one at the interaction site, but a certain similitude is observed in the MEP maps of all interacting molecules.

Figure 6 show the MEP maps of molecules HN31 and HN41. Figure 7 show the MEP maps of molecules HN38 and HN42.
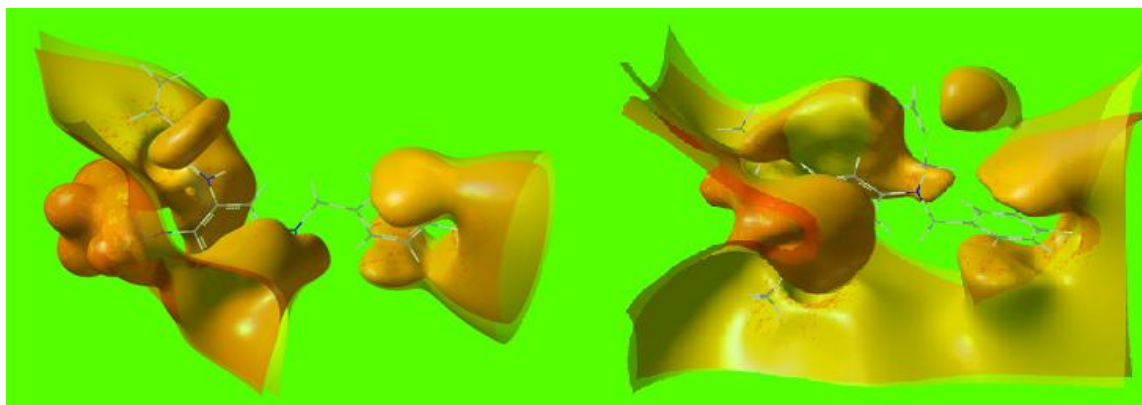
Figure 6: MEP map of molecules HN31 (left) and HN41 (right) (yellow isosurface = +0.0004, orange isosurface = -0.0004)
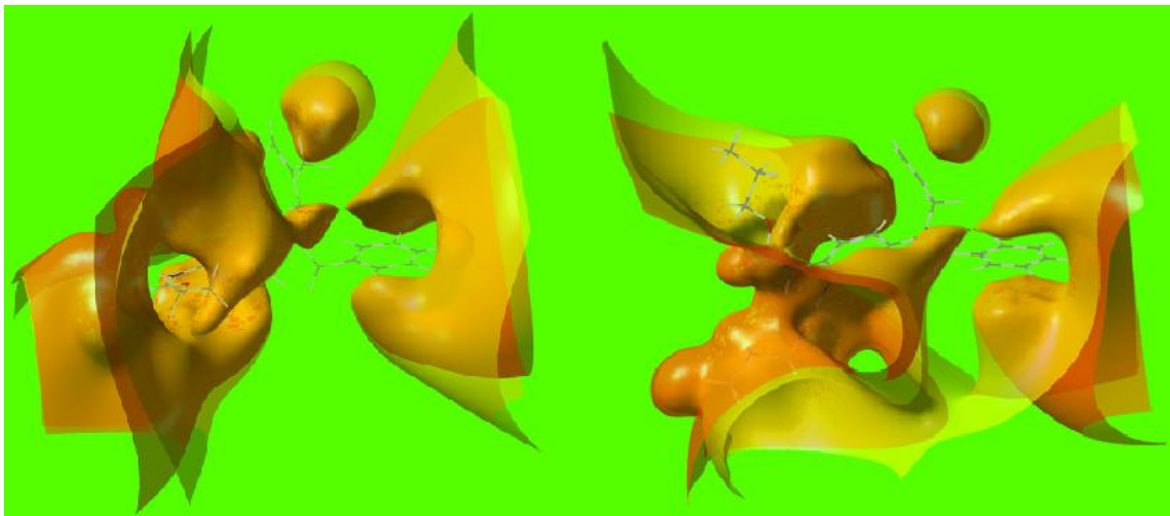
Figure 7: MEP map of molecules HN38 (left) and HN42 (right)(yellow isosurface = +0.0004, orange isosurface = -0.0004)

We can see that at the left and right sides of molecules there are volumes of negative MEPs. It is not possible to correlate a determinate MEP structure with a given activity, but the general similitude between the MEP maps is associated with the idea that they act at the same site and approach to it in the same orientation.

Discussion of results

The associated statistical parameters of Eq. 1 indicate that this equation is statistically significant and that the variation of the numerical values of a group of six local atomic reactivity indices of atoms of the common skeleton explains about 88 % of the variation of $\log(I/I_0)$.Table 2 shows that the importance of variables in Eq. 1 is$S_{10}^N(LUMO+2)^*>S_{21}^N(LUMO+1)^*\sim\eta_{27}>>F_{28}(LUMO+2)^*>S_{10}^E(HOMO-1)^*\sim s_{22}$.An enhanced inhibitory activity $(I/I_0 < 1)$ is our goal. Then, a high inhibitory activity is associated withsmall values of η_{27}, high positive values of $S_{10}^N(LUMO+2)^*$, $S_{21}^N(LUMO+1)^*$ and $F_{28}(LUMO+2)^*$, high negative values of $S_{10}^E(HOMO-1)^*$ and small values of s_{22}.Now, we shall employ the variable-by-variable analysis of each component of the QSAR equation.Atom 10 is a carbon in ring A (Fig. 2). Table 4 shows that the three lowest empty local MOs have a π nature.A high inhibitory activity is associated with high positive values of $S_{10}^N(LUMO+2)^*$. These values are obtained by lowering the energy of $(LUMO+2)_{10}^*$ making it more reactive [4]. This, in turn, will raise the reactivity of $(LUMO+1)_{10}^*$ and $(LUMO)_{10}^*$. Based on this result, we suggest that atom 10 is interacting with an electron-rich center through at least its three lowest empty local MOs. Given that this atom belongs to an aromatic system, the most probable interaction is a π-π one. The fact that high negative values of $S_{10}^E(HOMO-1)^*$ are also associated with high inhibitory activity seems to incontradiction with the above suggestion. We have two possible explanations. The first explanation considers that the beta value associated with $S_{10}^E(HOMO-1)^*$ is very low compared with the beta value associated with $S_{10}^N(LUMO+2)^*$. Therefore, we should not consider $S_{10}^E(HOMO-1)^*$ in the analysis. The other explanation is a theoretical one: atom 10 could be acting as a bridge between an electron-rich center and an electron-deficient center.Atom 21 is the first atom of the substituent attached to one of the COOR groups (a saturated carbon atom, seeFig. 2 and Table 1). Table 4 shows that all local MOs have aσ nature. High positive values of $S_{21}^N(LUMO+1)^*$ are needed for high inhibitory activity. These values are obtained by lowering the corresponding eigenvalue and making the MO more reactive. This suggests that atom 21 is interacting with an electron-rich center. The possible kinds of interactions are σ-σ or σ-π.Atom 27 is the first atom of the substituent attached to the other COOR group (a saturated carbon atom, see Fig. 2 and Table 1). Table 5 shows that all local MOs have aσ nature. Small values of small values of the local atomic hardness,η_{27}, are associated to high inhibitory activity. η_{27} corresponds to the $(HOMO)_{27}^*$-$(LUMO)_{27}^*$ gap and is a positive number (there are some exceptions). Table 5 shows that the local HOMO and the local LUMO are not the molecule's frontier MOs. Therefore for this case we have three ways to

lower the value of η_{27}: raise the $(HOMO)_{27}{}^*$ energy, lower the $(LUMO)_{27}{}^*$ energy or carry out both procedures simultaneously. These procedures produce very different changes in the local MO reactivity. Now, and considering the relative proximity of the NCOOR groups, we may hypothesize that atoms 21 and 27 could be interacting with the same electron-rich center. If this is the case, then the best approach to diminish the value of η_{27} is by lowering the $(LUMO)_{27}{}^*$ energy (and of $(LUMO+1)_{27}{}^*$ and/or $(LUMO+2)_{27}{}^*$ if necessary), making these MOs more reactive. Atom 28 is the first atom of the substituent attached to N-9 (a saturated carbon atom, see Fig. 2 and Table 1). Table 5 shows that all local MOs have a σ nature. A high inhibitory activity is associated with high positive values of $F_{28}(LUMO+2)^*$. This immediately suggests that atom 28 is interacting with an electron-rich center through at least its three lowest empty local MOs. Atom 22 is a nitrogen in the side chain attached to atom 14 (Fig 2).Small values of s_{22} are associated with high inhibitory activity. Considering that within the framework of the local atomic reactivity indices we are using $s_{22}=1/\eta_{22}$, we need to raise the value of η_{22}. As in the case of atom 27, we have three ways of doing this [4]. Table 4 shows that $(HOMO)_{22}{}^*$ coincides with the molecular HOMO in all cases but one and that all MOs have a π nature. Also we can see that $(LUMO)_{22}{}^*$ does not coincide with the molecular LUMO with one exception. Given the coincidence of the local frontier occupied MO with the molecular one, it seems that the appropriate way is to remove the localization of the molecular HOMO (and, if necessary, of other higher occupied molecular MOs) from atom 22. This procedure will raise the atomic net charge. In this is the case it is suggested that this atom is close to a negatively charged moiety in such a way that a decrease of the electronic density facilitates the interaction.All the above suggestions are displayed in the partial 2D pharmacophore of Fig. 8.
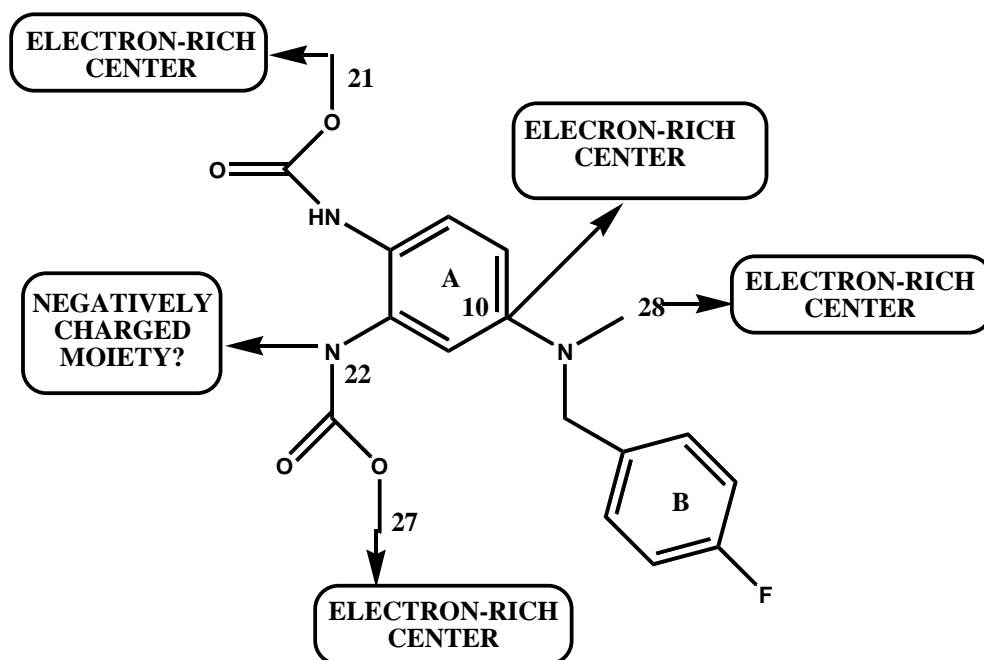
Figure 8: Partial 2D pharmacophore

Conclusions

In summary, we have obtained a statistically significant equation relating the variation of the KCNQ2 potassium channels inhibitory capacity of a series of retigabine derivatives with the variation of the numerical values of a set of local atomic reactivity indices belonging to some specific atoms. The corresponding partial pharmacophore was built from these results and it could serve as an aid to formulate new compounds with enhanced or diminished activity.

References

[1]. Luo, L.; Li, B.; Wang, S.; Wu, F.; Wang, X.; Liang, P.; Ombati, R.; Chen, J.; Lu, X.; Cui, J.; Lu, Q.; Zhang, L.; Zhou, M.; Tian, C.; Yang, S.; Lai, R. Centipedes subdue giant prey by blocking KCNQ channels. *Proc Natl Acad Sci U S A* 2018, 115, 1646-1651.

[2]. Hu, H. N.; Zhou, P. Z.; Chen, F.; Li, M.; Nan, F. J.; Gao, Z. B. Discovery of a retigabine derivative that inhibits KCNQ2 potassium channels. *Acta Pharmacologica Sinica* 2013, 34, 1359-1366.

[3]. Important. Given that the methodology used here has been employed in more than 50 papers, we have adopted a standard way to present some aspects of the research. Some phrases are stantart to all our papers because they cannot be written in infinite different ways. Do not confuse this with self plagiarism.

[4]. Gómez-Jeria, J. S.; Kpotin, G. Some remarks on the interpretation of the Local Atomic Reactivity Indices within the Klopman-Peradejordi-Gómez (KPG) Method. I. Theoretical Analysis. *Research Journal of Pharmaceutical, Biological and Chemical Sciences* 2018, 9, 550-561.

[5]. Gómez-Jeria, J. S. A New Set of Local Reactivity Indices within the Hartree-Fock-Roothaan and Density Functional Theory Frameworks. *Canadian Chemical Transactions* 2013, 1, 25-55.

[6]. Gómez-Jeria, J. S. *Elements of Molecular Electronic Pharmacology (in Spanish)*. 1st ed.; Ediciones Sokar: Santiago de Chile, 2013; p 104.

[7]. Gómez-Jeria, J. S. Modeling the Drug-Receptor Interaction in Quantum Pharmacology. In *Molecules in Physics, Chemistry, and Biology*, Maruani, J., Ed. Springer Netherlands: 1989; Vol. 4, pp 215-231.

[8]. Gómez-Jeria, J. S. On some problems in quantum pharmacology I. The partition functions. *International Journal of Quantum Chemistry* 1983, 23, 1969-1972.

[9]. Gómez-Jeria, J. S. 45 Years of the KPG Method: A Tribute to Federico Peradejordi. *Journal of Computational Methods in Molecular Design* 2017, 7, 17-37.

[10]. Kpotin, G. A.; Bédé, A. L.; Houngue-Kpota, A.; Anatovi, W.; Kuevi, U. A.; Atohoun, G. S.; Mensah, J.-B.; Gómez-Jeria, J. S.; Badawi, M. Relationship between electronic structures and antiplasmidial activities of xanthone derivatives: A 2D-QSAR approach. *Structural Chemistry, https://doi.org/10.1007/s11224-019-01333-w* 2019.

[11]. Gómez-Jeria, J. S.; Sánchez-Jara, B. An introductory theoretical investigation of the relationships between electronic structure and A1, A2A and A3 adenosine receptor affinities of a series of N6-8,9-trisubstituted purine derivatives. *Chemistry Research Journal* 2019, 4, 46-59.

[12]. Gómez-Jeria, J. S.; Gatica-Díaz, N. A preliminary quantum chemical analysis of the relationships between electronic structure and $5-HT_{1A}$ and $5-HT_{2A}$ receptor affinity in a series of 8-acetyl-7-hydroxy-4-methylcoumarin derivatives. *Chemistry Research Journal* 2019, 4, 85-100.

[13]. Kpotin, G.; Gómez-Jeria, J. S. Quantum-Chemical Study of the Relationships between Electronic Structure and Anti-Proliferative Activities of Quinoxaline Derivatives on the K562 and MCF-7 Cell Lines. *Chemistry Research Journal* 2018, 3, 20-33.

[14]. Kpotin, G.; Gómez-Jeria, J. S. A Quantum-chemical Study of the Relationships Between Electronic Structure and Anti-proliferative Activity of Quinoxaline Derivatives on the HeLa Cell Line. *International Journal of Computational and Theoretical Chemistry* 2017, 5, 59-68.

[15]. Frisch, M. J.; Trucks, G. W.; Schlegel, H. B.; Scuseria, G. E.; Robb, M. A.; Cheeseman, J. R.; Montgomery, J., J.A.; Vreven, T.; Kudin, K. N.; Burant, J. C.; Millam, J. M.; Iyengar, S. S.; Tomasi, J.; Barone, V.; Mennucci, B.; Cossi, M.; Scalmani, G.; Rega, N. *G03 Rev. E.01*, Gaussian: Pittsburgh, PA, USA, 2007.

[16]. Gómez-Jeria, J. S. *D-Cent-QSAR: A program to generate Local Atomic Reactivity Indices from Gaussian 03 log files. v. 1.0*, v. 1.0; Santiago, Chile, 2014.

[17]. Gómez-Jeria, J. S. An empirical way to correct some drawbacks of Mulliken Population Analysis (Erratum in: J. Chil. Chem. Soc., 55, 4, IX, 2010). *Journal of the Chilean Chemical Society* 2009, 54, 482-485.

[18]. 18. Statsoft. *Statistica v. 8.0*, 2300 East 14 th St. Tulsa, OK 74104, USA, 1984-2007.

[19]. Hanwell, M.; Curtis, D.; Lonie, D.; Vandermeersch, T.; Zurek, E.; Hutchison, G. Avogadro: an advanced semantic chemical editor, visualization, and analysis platform. *Journal of Cheminformatics* 2012, 4, 17.